

Original Article

Effect of subarachnoid hemorrhage on voltage-dependence calcium channel current in cerebral artery smooth muscle cells

Fei Wang, Yong Wang, Li Zhang, Huan-Zhi Wang, Hua-Lin Yu

The Second Department of Neurosurgery, First Affiliated Hospital of Kunming Medical University, Kunming 650032, China

Received June 23, 2015; Accepted August 8, 2015; Epub August 15, 2015; Published August 30, 2015

Abstract: Objective: To investigate the effect of subarachnoid hemorrhage (SAH) on voltage-dependent calcium channel (VDCC) current in cerebral artery smooth muscle cells (SMCs), oxyhemoglobins (OxyHb) concentration and vasospasm. Method: Thirty-six clean SD rats were used to establish SAH model by injecting autologous arterial blood into suprasellar cistern with the aid of stereotaxic instrument. They were divided into arterial SAH group (14 rats), venous SAH group (13 rats) and sham operation group (9 rats), and OxyHb concentrations were measured in the first two groups. Relative membrane surface area of cerebral artery SMCs, resting potential and VDCC current were measured using a patch clamp at day 3 after modeling; cerebral blood flow (CBF) was measured by using fluorescent microsphere-based lateral flow assay. Results: OxyHb concentration of arterial SAH group (127 ± 4 g/L) was higher than that of venous SAH group (54 ± 6 g/L) and sham operation group (50 ± 5 g/L), with significant difference ($P < 0.05$); The maximum VDCC current (3.22 ± 0.31 pA/pF) of the arterial SAH group was obviously higher than that of venous SAH group (2.19 ± 0.27 pA/pF) and sham operation group (2.18 ± 0.29 pA/pF), also showing a significant difference ($P < 0.05$). For arterial SAH group, VDCC current consisted of L- and R-type calcium current, and for venous SAH group the VDCC current consisted of L-type calcium current; CBF of arterial SAH group (0.83 ± 0.14 ml/g/min) was significantly higher than that of venous SAH group (1.28 ± 0.28 ml/g/min) and sham operation group (1.35 ± 0.19 ml/g/min) ($P < 0.05$). Conclusion: The effect of arterial SAH was greater on the expression and function of VDCCs in cerebral artery SMCs than venous SAH. This may be explained by the differences in the concentration and composition of pathogenic agents for vasospasm in the arterial and venous blood, such as OxyHb.

Keywords: Subarachnoid hemorrhage (SAH), cerebral artery, voltage-dependent calcium channel (VDCC), patch clamp, oxyhemoglobins (OxyHb), rats

Introduction

The incidence of subarachnoid hemorrhage (SAH) is about 1/10000 per year. SAH is divided into arterial SAH and venous SAH by the type of offending blood vessels [1]. The former accounts for about 85% of SAH, with intracranial aneurysm, ruptured arteriovenous malformations and brain tumor apoplexy as the main causes; the latter is primarily caused by intracranial venous thrombosis and venous sinus thrombosis, coagulation disorder and non-aneurysmal SAH near the midbrain [2]. Venous SAH is characterized by mild symptoms, low incidence of cerebral vasospasm and good prognosis [3]. It is shown that SAH has an inhib-

itory effect on KV current in SMCs of the cerebral cortex and perforator artery [4]. Since the diameter, tension and blood flow of the blood vessels are regulated by VDCC current, VDCC current is also associated with cerebral vasospasm [5]. VDCC current can be regulated by the decomposition products of red blood cells accumulating in the subarachnoid cavity after SAH and other components in blood. Shi et al. [6] have demonstrated that VDCC current after arterial SAH is enhanced by about 150%. We investigated the sensitivity of arterial and venous SAH to cerebral vasospasm and the differences in the regulatory effects of different components in venous and arterial blood on VDCC current. The findings on the differences in

Subarachnoid hemorrhage on VDCC

VDCC current, resting potential of SMCs and CBF regulation between arterial SAH and venous SAH shed new light into the treatment of SAH.

Materials and methods

Establishment of rat model of SAH and grouping

Thirty-six SD rats regardless of sex, weighted 300-350 g, were provided by Experimental Animal Center of Kunming Medical University (SCXK (Yunnan) 2011-0004). They were divided into arterial SAH group (14 rats), venous SAH group (13 rats) and sham operation group (9 rats) by using a random number table. SAH model was then established by the injection of autologous venous blood into the suprasellar cistern using the stereotaxic instrument [7]. The rats were fasted for 1 d before surgery. After intraperitoneal injection of 10% chlorate hydrate (0.4 ml/100 g), the right groin area was cut open to expose femoral artery and vein. The femoral artery (arterial SAH group) or the femoral vein (venous SAH group) was punctured using sterile remaining needles (24 G), and 4.5 ml of blood sample was drawn for blood gas analysis and cisternal injection.

Excision was performed along the scalp midline, and the periosteum and temporal muscles were stripped away. The head of the rats was fixed on the stereotaxic instrument, with anterior fontanelle placed on the same level as lambda. A 1.5 mm hole was drilled at 7.0 mm in front of the anterior fontanelle along the sagittal midline. Puncture was done at this site using No. 7 needle, with the needle tail inclining forwards by 30°. Clear cerebrospinal fluid was drawn after the needle was inserted to the depth of 8-9 mm. With the needle entering the subarachnoid cavity, 0.25 ml autologous blood (without anticoagulant) was injected for 12 s. For the sham operation group, equal volume of sterile isotonic saline solution was injected by the same method. After modeling, the rats showed signs of listlessness, drowsiness, reduced movement, and some even showed movement disorder. No rats died during experiment.

Determination of OxyHb concentration

Blood gas analyzer (Texas Instrument, USA) was used to determine OxyHb concentrations

in the arterial or venous blood of arterial SAH group and venous SAH group at 3 d after modeling, respectively.

Neural deficit scores

Neural deficit scores were assessed using Garcia scale [8] at day 3 after modeling (the highest and lowest scores were 18 and 3, respectively).

Isolation of arterial and venous SMCs

After assessment of neural deficit scores, 10% chloral hydrate (0.4 ml/100 g) was injected intraperitoneally, and the rats showed no corneal reflex or pain-escaping behavior. The rats were sacrificed by cervical dislocation. The tissues were harvested and preserved in artificial cerebrospinal fluid at low temperature. Sharp separation of middle cerebral artery was carried out under the microscope. Then the tissues were successively digested with solution I containing 0.3 mg/mL papain (Worthington, USA) + 0.7 mg/ml dithioerythritol (Sigma, USA) and solution II containing 0.7 mg/mL collagenase type F (Sigma, USA) + 0.3 mg/ml collagenase type H (Sigma, USA) for 17 min (37°C water bath). After digestion, the tissues were transferred to glutamate solution and gently blown for about 1 min to disperse the SMCs [9].

Cell viability detection

To ensure the reliability of further experiments, viability was first detected for SMCs. The cell suspension above was mixed with 0.4% trypan blue solution (Gibco, USA) in the proportion of 9:1. The cells were counted under the inverted microscope in high-power field of vision so as to determine the cell membrane integrity and percentage of viable cells. Viable cells and integral membranes were not stained, while the dead cells were stained blue. Cell viability was measured by the percentage of viable cells: Percentage of viable cells (%) = Total number of viable cells/(total number of viable cells + total number of dead cells)×100%.

Preparation of glass microelectrodes

Glass electrode blank made of borosilicate with outer diameter of 1.50 mm and inner diameter of 1.17 mm (Sutter Instrument, USA) was soaked in methanol and dried. The glass microelectrodes were drawn using PC-10 microelec-

Subarachnoid hemorrhage on VDCC



Figure 1. Cerebral artery smooth muscle cells and micro electrode form whole cell patch clamp recording mode ($\times 200$).

trode puller (Narishige, Japan) and then processed into outer diameter of about $1 \mu\text{m}$ at the tip using MF-830 microforge (Narishige, Japan), with resistance of 3-5 $\text{M}\Omega$.

Resting potential determination

The suspension of arterial SMCs was added into the water bath tank of the microscope (Leica, Germany). The cells adhered to the wall, and those with slender morphology and good refractivity were chosen. The tip of glass microelectrodes formed a high-resistance seal with the cells, and the membranes were quickly ruptured (**Figure 1**). Axopatch200B patch clamp amplifier (Axon, USA) was used to determine the resting potential in current-clamp mode ($I=0$, METER:Vm). The composition of extracellular fluid was 125 mmol/L NaCl, 2 mmol/L CaCl_2 (bivalent cation carriers), 5 mmol/L KCl, 10 mmol/L HEPES, 1 mmol/L MgCl_2 , 10 mmol/L glucose. The pH value was adjusted to 7.4 using NaOH solution. The composition of intracellular fluid was 130 mmol/L CsCl, 10 mmol/L EGTA, 10 mmol/L HEPES, 1 mmol/L MgCl_2 , 2 mmol/L adenosine triphosphate (ATP), 0.5 mmol/L guanosine triphosphate (GTP), 5 mmol/L creatine phosphate, 10 mmol/L glucose. The pH value was adjusted to 7.2 with CsOH.

VDCC current recording

After the rupture of cell membranes and in whole-cell recording mode, VDCC current was recorded with the voltage clamp (V-CLAMP, METER:I) and pulse voltage program. The val-

ues of membrane capacity (in direct proportion to membrane surface area) were read from the amplifier. The compositions of extracellular fluid and intracellular fluid were the same as above. Nifedipine (blocker of L-VDCCs) and SNX-482 (blocker of R-type VDCCs) were prepared on the day of experiment using extracellular fluid. Patch clamp recording was carried out under room temperature ($20\text{-}22^\circ\text{C}$) with the use of perfusion system.

CBF determination by fluorescent microsphere-based lateral flow assay

After assessment of neural deficit scores and general anesthesia, the left groin was cut open, and the ipsilateral femoral artery and vein were punctured and connected with a microinjector. Percutaneous left ventricular puncture was carried out above the xiphoid process. While drawing the femoral artery blood at constant rate, 3 ml of fluorescent microspheres were injected into the left ventricle (Molecular Probes Inc., USA). The rats were sacrificed, and the brain tissues were harvested and weighed. For every gram of brain tissues or arterial blood, 3-4 ml of 4 mmol/L KOH was added for digestion for 48 h. The tissues were filtered (pore size of filter membrane $5 \mu\text{m}$, microsphere diameter $15 \mu\text{m}$) so that the microspheres were captured on the filter membrane. Fluorescence intensity was measured with a fluorescence spectrophotometer, and absolute CBF was calculated [7].

Statistical analysis

Statistical analysis was done using Prism 6.0 software. Measurement data were expressed as $\bar{x} \pm s$, with n representing cell count and N the number of rats. Viability of SMCs between the groups was compared by Chi-square test; OxyHb concentration of the two groups was analyzed using t-test, average relative membrane surface area and resting potential by one-way ANOVA, and average current density by multivariate analysis of variance (MANOVA). The means of the two groups were compared by using q test. $P < 0.05$ indicated significant differences.

Results

OxyHb concentration (g/L)

OxyHb concentration of arterial SAH group, venous SAH group and sham operation group

Subarachnoid hemorrhage on VDCC

Table 1. OxyHb concentration and neural deficit scores ($\bar{x} \pm s$)

	N	OxyHb concentration (g/L)	Neural deficit scores
Arterial SAH	14	127±4	17.41±0.22
Venous SAH	13	54±6	17.53±0.10
Sham operation	9	54±5	18.00±0.00
F value		23872.28	54.74
P value		0.00	0.00

Table 2. Relative membrane surface area of SMCs ($\bar{x} \pm s$)

	Arterial SAH	Venous SAH	Sham operation
n	24	19	29
Relative membrane surface area	12.2±1.0	14.8±1.0	15.2±0.7

$F=80.62$, $P<0.05$; q test, comparison between Arterial SAH and Sham operation, $q=16.99$, $P<0.05$; comparison between Arterial SAH and Venous SAH, $q=13.42$, $P<0.05$; comparison between Venous SAH and Sham operation, $q=1.92$, $P>0.05$.

Table 3. Resting potential of SMCs ($\bar{x} \pm s$)

	Arterial SAH	Venous SAH	Sham operation
n	11	8	14
Resting potential	37.9±1.2	52.2±1.3	51.5±1.7

$F=324.09$, $P<0.05$; q test, comparison between Arterial SAH and Sham operation, $q=32.37$, $P<0.05$; comparison between Arterial SAH and Venous SAH, $q=29.50$, $P<0.05$; comparison between Venous SAH and Sham operation, $q=1.50$, $P>0.05$.

was 127±4 g/L, 54±6 g/L and 50±5 g/L, respectively, indicating significant differences between the groups ($F=23872.28$, $P<0.05$). OxyHb concentration of arterial SAH group was obviously higher than that of venous SAH group and sham operation group ($P<0.05$), with no significant differences between arterial SAH group and sham operation group ($P>0.05$).

Neural deficit scores

Before modeling, the neural deficit scores of rats were all 18. Neural deficit scores of arterial SAH group, venous SAH group and sham operation group were 17.41±0.22 (N=14), 17.53±0.10 (N=13) and 18.00±0.00 (N=9) at 3 d after modeling, respectively, which indicated significant differences ($F=54.74$, $P<0.05$). The neural deficit scores of arterial SAH group and venous SAH group decreased compared with the sham operation group ($P<0.05$); arterial SAH group and venous SAH group showed no significant difference ($P>0.05$, **Table 1**).

Percentage of viable cells (%)

In high-power field of vision, the percentage of viable cells (%) in arterial SAH group, venous SAH group and sham operation group was 83.1±3.0%, 86.7±2.2% and 84.6±3.9%, respectively; the three groups did not differ considerably ($F=1.18$, $P>0.05$).

Relative membrane surface area of SMCs

Cell membrane capacitance is in direct proportion to membrane surface area, and it represents relative membrane surface area. Relative membrane surface area of SMCs in arterial SAH group, venous SAH group and sham operation group was 12.2±1.0 (n/N=24/6), 14.8±1.0 (n/N=19/6) and 15.2±0.7 (n/N=29/4), respectively, and the differences were of statistical significance ($F=80.62$, $P<0.05$). Relative membrane surface area of SMCs in arterial SAH group was considerably smaller than that of venous SAH group and sham operation group ($P<0.05$), with no significant differences

observed between arterial SAH group and sham operation group ($P>0.05$, **Table 2**).

Resting potential (mV)

Resting potential of SMCs in arterial SAH group, venous SAH group and sham operation group was 37.9±1.2 mV (n/N=11/6), 52.2±1.3 mV (n/N=8/6) and 51.5±1.7 mV (n/N=14/4), respectively; the three groups differed remarkably ($F=324.09$, $P<0.05$). The resting potential of arterial SAH group was obviously lower than that of venous SAH group and sham operation group ($P<0.05$), but venous SAH group did not differ considerably from the sham operation group ($P>0.05$, **Table 3**).

Effect of VDCC current density (pA/pF) and calcium channel blocker

VDCC current was evoked by voltage step in whole-cell recording mode. The membrane potential (V_m) was depolarized discontinuously

Subarachnoid hemorrhage on VDCC

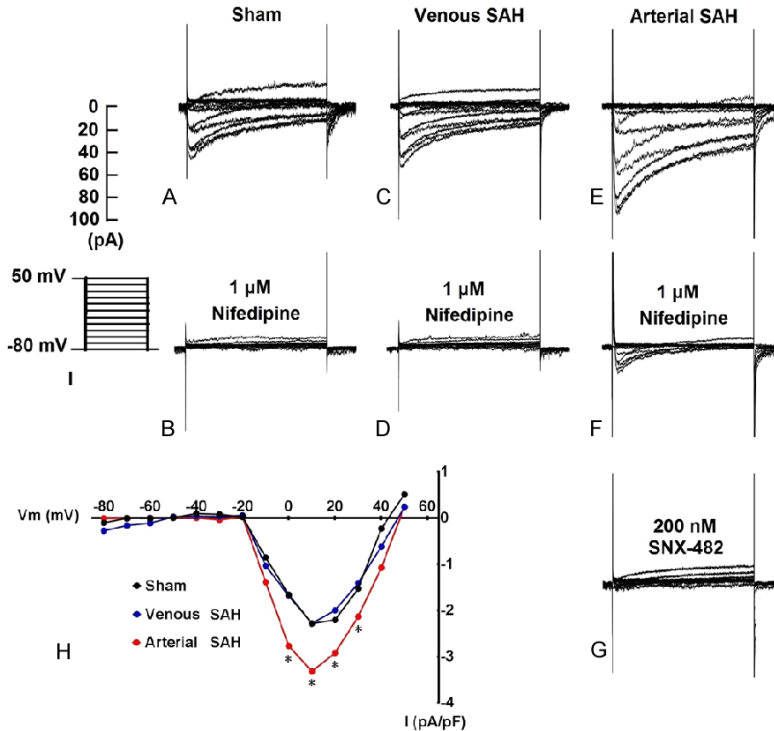


Figure 2. VDCCs current density (pA/pF) as well as the role of calcium channel blockers.

Table 4. VDCC current density (pA/pF) ($\bar{x} \pm s$)

	Arterial SAH	Venous SAH	Sham operation
n	15	13	11
Current density	3.22±0.31	2.19±0.27	2.18±0.29

$F=580.99$, $P<0.05$; q test, comparison between Arterial SAH and Sham operation, $q=12.84$, $P<0.05$; comparison between Arterial SAH and Venous SAH, $q=13.18$, $P<0.05$; comparison between Venous SAH and Sham operation, $q=0.11$, $P>0.05$.

Table 5. CBF ($\bar{x} \pm s$)

	Arterial SAH	Venous SAH	Sham operation
n	8	7	5
CBF	0.83±0.14	1.28±0.28	1.35±0.19

$F=10.83$, $P<0.05$; q test, comparison between Arterial SAH and Sham operation, $q=6.21$, $P<0.05$; comparison between Arterial SAH and Venous SAH, $q=5.97$, $P<0.05$; comparison between Venous SAH and Sham operation, $q=0.77$, $P>0.05$.

to 50 mV from -80 mV at an amplitude of 10 mV. Each voltage step lasted 800ms, followed by repolarization to -80 mV. VDCC current of venous SAH group and sham operation group could be completely blocked by 1 μM nifedipine, while about 20% of the current was left unblocked in arterial SAH group; this portion of

current was then completely blocked by 200 nM SNX-482 (Figure 2). This indicated that VDCC current in venous SAH group and sham operation group consisted only of L-VDCC current, while the current in arterial SAH group consisted of L-type and R-type VDCC current. Maximum VDCC current (pA) was obtained for all three groups at $V_m = 10$ mV, with the value of 3.22 ± 0.31 pA ($n/N=15/4$), 2.19 ± 0.27 pA ($n/N=13/6$) and 2.18 ± 0.29 pA ($n/N=11/6$), respectively; the three groups showed statistically significant differences ($F=580.99$, $P<0.05$). With $V_m = 0-30$ mV, VDCC current density of arterial SAH group was obviously higher than that of venous SAH group and sham operation group ($P<0.05$). Venous SAH group and sham operation group did not show significant difference in VDCC current density within the experimental range of membrane potential ($P>0.05$, Table 4).

CBF (ml/g/min)

CBF of arterial SAH group, venous SAH group and sham operation group was 0.83 ± 0.14 ml/g/min ($N=8$), 1.28 ± 0.28 ml/g/min ($N=7$) and 1.35 ± 0.19 ml/g/min ($N=5$), respectively; the differences between the three groups were of statistical significance ($F=10.83$, $P<0.05$). CBF of arterial SAH group was obviously lower than that of venous SAH group and sham operation group ($P<0.05$); venous SAH group and sham operation group did not show statistically significant difference in CBF ($P>0.05$, Table 5).

Discussion

Cerebral vasospasm is one common complication of SAH and also one cause of SAH-related death. Severe hemorrhage at early stage can lead to a rapid increase of intracranial pressure

and a decline of vascular regulation. The autonomic nerve ending will produce cerebral vasospasm under stimulation. As OxyHb is released from the hematocoele in subarachnoid cavity, free radicals and lipid peroxide are generated, which affect the metabolism of arachidonic acid and facilitate the release of endothelin. Therefore, cerebral vasospasm persists. Experimental results indicate that cell apoptosis usually ensues after cerebral vasospasm in SAH [10]. Cell apoptosis of the greatest severity occurs in the involved vascular endothelial cells, followed by hypothalamic neural cells, and the least in the cerebral cortex. Cell apoptosis in vascular walls with spasm plays an important role in the formation mechanism of cerebral vasospasm. The techniques available at present can only reduce ischemia induced by cerebral vasospasm, so the prevention of cerebral vasospasm is very important. Most cerebral vasodilators may cause the simultaneous rise of blood pressure and intracranial pressure. Cerebral perfusion will decrease instead of increasing, which is more life-threatening. According to some foreign studies [11], mRNA of R-type calcium channel is upregulated at day 5 after SAH, and SNX-482 effectively decreases the inflow of calcium ions into cerebral SMCs while counteracts the blood vessel contraction induced by SAH. Our preliminary study has demonstrated that SNX-482 partially restores the decline of CBF induced by SAH [12]. Adverse changes of cells following SAH can be alleviated by improving CBF, thereby reducing the complications and prognosis of SAH [13].

We showed that arterial SAH caused the VDCC current intensity of cerebral artery SMCs to increase alongside the changes of VDCC current composition compared with normal SMCs [12]. Meanwhile, CBF decreased significantly. In contrast, no such changes were observed in venous SAH, which could be explained by the differences in OxyHb concentration. The reduction of membrane surface area of SMCs in arterial SAH may be associated with intensified isotonic contraction of SMCs. In normal cerebral artery that expresses only L-VDCCs, VDCC current can be completely blocked by nifedipine. As shown by the preliminary study, arterial SAH induced the expression of R-type VDCCs in cerebral artery SMCs [14]. Part of the current could not be blocked by nifedipine in arterial SAH, but by SNX-482, the blocker of R-type cal-

cium channel. Further analysis indicated that R-type VDCCs were upregulated in the arterial blood but not in the venous blood. Thus, for arterial SAH, the combined use of L-type and R-type calcium channels blockers can completely block the inflow of calcium ions, therefore eliminating or relieving vasospasm [15]. OxyHb is a pathogenic agent of cerebral vasospasm, and OxyHb concentration in cerebrospinal fluid is associated with the severity of vasospasm. Because the venous oxygen saturation is only about 40% of the arterial oxygen saturation, the venous OxyHb concentration is 35%-45% of the arterial OxyHb concentration [16], which corresponds to the finding of this study. OxyHb concentration in the cerebrospinal fluid at day 7 after the onset of arterial SAH was about 70 $\mu\text{mol/L}$. The fluctuation of OxyHb concentration was also consistent with the time course of cerebral vasospasm [17]. We did not detect OxyHb concentration in the cerebrospinal fluid due to the lack of appropriate method to collect enough cerebrospinal fluid from animals. The clearing effect of cerebrospinal fluid circulation on OxyHb may partially account for the absence of depolarization of SMCs and the decline of CBF using the venous blood. Vascular reaction will not be activated obviously unless OxyHb concentration reaches a certain threshold. This may be associated with the apoptosis of endothelial cells induced by G protein-coupled receptor. Various mechanisms are involved in the hyperpolarization of vascular SMCs. After the apoptosis of endothelial cells, VDCC current will be intensified due to depolarization of vascular SMCs. Besides OxyHb, other pathogenic agents of vasospasm also show concentration differences, including bilirubin and endothelin. However, there are still no studies on the concentration and metabolism of these factors in cerebrospinal fluid [18].

Venous SAH has a much better prognosis than arterial SAH. In addition to the difference in susceptibility to vasospasm contributed by components of blood, the following reasons are identified: Venous SAH has a smaller blood loss, and the involvement of many cisterns is rare; Recurrence of venous SAH is extremely rare, and only a few cases of recurrent venous SAH have been reported worldwide; Venous SAH mainly takes place in infratentorial cistern and the sulci on the convex surface of the brain, which are distant away from Willis loop.

Therefore, less interference is caused to the important intracranial arteries; Venous SAH is rarely combined with intracranial complications such as hydranencephaly [19].

The differences in VDCC current, resting potential of SMCs and CBF between arterial SAH and venous SAH explain different clinical features of the two types of SAH. On this basis, we can find the treatment targets and thus improve the prognosis of SAH. However, the large difference of the sample size between the groups reduced the accuracy of statistical analysis, since many data of patch clamp recordings were removed due to background noise. For future studies, automatic patch clamping featured by lower noise and more stable seal will be developed to overcome these defects, so that the research can be improved in terms of accuracy and objectivity.

Acknowledgements

This work was supported by the National Natural Science Foundation of China (No. 81260182); Natural Science Foundation of Yunnan Province (No. 2012FB036).

Disclosure of conflict of interest

None.

Address correspondence to: Hua-Lin Yu, First Affiliated Hospital of Kunming Medical University, 295 Xichang Rd, Kunming 650032, Yunnan, China. Tel: +86- 0871-65324888; Fax: +86- 0871-65324888; E-mail: yuhalini@163.com

References

- [1] Greving JP, Wermer MJ, Brown RD Jr, Morita A, Juvela S, Yonekura M, Ishibashi T, Torner JC, Nakayama T, Rinkel GJ and Algra A. Development of the PHASES score for prediction of risk of rupture of intracranial aneurysms: a pooled analysis of six prospective cohort studies. *Lancet Neurol* 2014; 13: 59-66.
- [2] Cheng SL, Ren AZ, Duan CZ, Zhong PB and Li TL. Etiological diagnosis and interventional therapy of spontaneous subarachnoid hemorrhage. *Chinese Journal of Neuromedicine* 2006; 5: 1160-1162.
- [3] Prat D, Goren O, Bruk B, Bakon M, Hadani M and Harnof S. Description of the vasospasm phenomena following perimesencephalic non-aneurysmal subarachnoid hemorrhage. *Bio-med Res Int* 2013; 2013: 371063.
- [4] Wang F, Wang HZ, Li SP, Sun T, Ma YL and Yu HL. The different suppression on voltage-dependent potassium channels currents of smooth muscle cells from cerebral pial arteries and penetrating arteries by subarachnoid hemorrhage. *Chinese Journal of Neurology* 2014; 47: 1-5.
- [5] Wang F, Yin YH, Jia F and Jiang JY. Antagonism of R-type calcium channels significantly improves cerebral blood flow after subarachnoid hemorrhage in rats. *J Neurotrauma* 2010; 27: 1723-1732.
- [6] Shi X, Fu Y, Liao D, Chen Y and Liu J. Alterations of voltage-dependent calcium channel currents in basilar artery smooth muscle cells at early stage of subarachnoid hemorrhage in a rabbit model. *PLoS One* 2014; 9: e84129.
- [7] Wang F, Yin YH, Jia F and Jiang JY. Effect of R-type calcium channel antagonist on contractile-related proteins in cerebral artery following subarachnoid hemorrhage in rats. *Chinese Journal of Cerebrovascular Diseases* 2003; 18: 24-28.
- [8] Garcia JH, Wagner S, Liu KF and Hu XJ. Neurological deficit and extent of neuronal necrosis attributable to middle cerebral artery occlusion in rats. Statistical validation. *Stroke* 1995; 26: 627-634.
- [9] Koide M, Wellman GC. SAH-induced suppression of voltage-gated potassium channel currents in parenchymal arteriolar myocytes involves activation of the HB-EGF/EGFR pathway. *Acta Neurochir Suppl* 2013; 115: 179-184.
- [10] Park S, Yamaguchi M, Zhou C, Calvert JW, Tang J and Zhang JH. Neurovascular protection reduces early brain injury after subarachnoid hemorrhage. *Stroke* 2004; 35: 2412-2417.
- [11] Ishiguro M, Wellman TL, Honda A, Russell SR, Tranmer BI and Wellman GC. Emergence of a R-type Ca²⁺ channel (Ca_v 2.3) contributes to cerebral artery constriction after subarachnoid hemorrhage. *Circ Res* 2005; 96: 419-426.
- [12] Wang F, Yin YH, Fu J, Zhang SL, Guo LM, Chen QS and Jiang JY. Effect of R-type Calcium Channel Antagonist on Cerebral Blood Flow Following Subarachnoid Hemorrhage. *Chinese Journal of Clinical Neurosciences* 2010; 18: 24-28.
- [13] Sen J, Belli A, Albon H, Morgan L, Petzold A and Kitchen N. Triple-H therapy in the management of aneurysmal subarachnoid hemorrhage. *Lancet Neurol* 2003; 2: 614-621.
- [14] Wang F, Wang HZ, Yao XY, Sun T, Ma YL and Yu HL. The specific study of voltage-dependent calcium channels currents in rats cerebral arteries myocytes. *Chinese Journal of Neurosurgery* 2014; 30: 945-948.
- [15] Li P, Wu JM, Chu ZH and Liu CM. 6-amino caproic acid and nim horizon joint clinical re-

Subarachnoid hemorrhage on VDCC

- search for the treatment of subarachnoid hemorrhage. *Journal of Clinical Neurology* 2003; 16: 243.
- [16] Zavorsky GS, Cao J, Mayo NE, Gabbay R and Murias JM. Arterial versus capillary blood gases: a meta-analysis. *Respir Physiol Neurobiol* 2007; 15: 268-279.
- [17] Wu DM, Guan YX, Ju XY, Liao YH, Lu Z, Li J, Wang HB and Ding JR. Analysis on the Relationship of Endothelin and Oxyhemoglobin to Cerebral Vasospasm in Patients with Subarachnoid Hemorrhage. *Journal of Guiyang Medical College* 2013; 37: 629-631.
- [18] Pyne-Geithman GJ, Nair SG, Stamper DN and Clark JF. Role of bilirubin oxidation products in the pathophysiology of DIND following SAH. *Acta Neurochir Suppl* 2013; 115: 267-273.
- [19] Hu JQ, Lin D, Shen JK, Zhao WD and Lin HW. Perimesencephalic nonaneurysmal subarachnoid hemorrhage: diagnosis and treatment. *Chinese Journal of Neuromedicine* 2003; 2: 170-172.